

Air Nonlinear dynamics triggered by an ultra-intense THz bullet

Mostafa Shalaby¹ and Christoph P. Hauri^{1,2}

¹Paul Scherrer Institute, SwissFEL, 5232 Villigen PSI, Switzerland.

²École Polytechnique Fédérale de Lausanne, 1015 Lausanne, Switzerland.

*Correspondence to: most.shalaby@gmail.com and christoph.hauri@psi.ch

Air turns into a nonlinear medium for electromagnetic waves under exceptionally strong fields. However up to present, its minuscule nonlinear response has limited the exploration to the optical frequency regime owing to the availability of intense near-infrared lasers. Here, we report on the observation of large-amplitude nonlinearity in air induced by an extremely intense light bullet at Terahertz frequencies (0.1-10 THz) provoking strong air birefringence. The observed nonlinearity manifests itself as third order susceptibility. The presented nonlinear observations break the barrier for the entire exciting THz-induced nonlinear phenomena in air ranging from THz-induced self-focusing and self-phase modulation to THz solitons and filamentation.

Electric susceptibility χ describes the ability of a medium to react and relocate its electronic distribution in an external electric field E , with air being among the hardest to polarize. On the microscopic scale, a constant E deforms (displaces) the electric clouds in the atoms, inducing static dipoles. This process is usually counteracted by a recovery force from the (oppositely charged) nucleus. An oscillating laser field induces an oscillating moment. Macroscopically, this leads to a time-dependent polarization $P(t): \chi E(t)$. At extremely intense electric fields, the induced polarization response makes the recovery process depend nonlinearly on the induced deformation force. This process is largely responsible for nonlinear properties of matter with intense laser pulses leading, for example, to the

emission of electromagnetic radiation in spectral regions far away from the initial laser spectrum (1,2).

In contrast to solids, air molecules have nearly vanishing average linear susceptibility $\chi^{(1)}$ of 5.4×10^{-4} . In gases, the third order susceptibility $\chi^{(3)}$ is the first nonlinear susceptibility term which is present, due to symmetry constraints. However, $\chi^{(3)}$ of air is extremely weak, being $8.8 \times 10^{-26} \text{ m}^2/\text{V}^2$ (3). Observation of nonlinearities in air requires therefore intensities on the order of PW/m^2 which is being limited to date to intense lasers emitting visible-near infrared radiation ($\sim 400 \text{ THz}$). While at optical frequencies, a multitude of nonlinear phenomena such as self-focusing (4), third harmonic generation (1,2), soliton formation (5), and many others were induced by coupling the laser electric field to the polarization by $\chi^{(3)}$ the nonlinear properties of air at low frequencies, and related phenomena are completely unexplored, as THz technology has severely lagged behind the required intensities (6-9). Recent progress in source developments (10) enabled some observations of nonlinear spectroscopy in solids (11-14) but has yet prevented any demonstration of THz-induced nonlinearity in air. This leaves the scientifically and technologically appealing THz-driven nonlinear applications completely unexplored, ranging from long-distance atmospheric sensing, filamentation, high-order harmonic generation to soliton formation and supercontinuum generation. Here, we use a newly developed THz bullet to trigger air nonlinearity (15) in this unexplored frequency region.

A change in the electronic susceptibility can be experimentally determined by measuring the refractive index n . In a centro-symmetric material, they are related (1,2) by

$$n = (\chi + 1)^{1/2} = (\chi^{(1)} + 1)^{1/2} + \frac{3\chi^{(3)}}{8n_0} |E^{\text{THz}}|^2 = n_0 + n_2 I \quad (1)$$

where n_0 and I are the linear refractive index and peak intensity of the exciting field. n_2 is the nonlinear refractive index, commonly referred to as Kerr coefficient. In order to measure the THz-induced nonlinearity, we performed THz pump-optical probe spectroscopy (Fig. 1A). Our THz trigger consists of a λ^3 THz bullet (i.e. a diffraction-limited and transform-limited single-cycle pulse) with maximum electric and magnetic field strengths of 3.3 GV/m and 11 T , respectively at 3.9 THz center frequency (15). The

corresponding peak intensity is 14.4 PW/m^2 . The probe pulses are 800 nm-centered pulses polarized at 45° with respect to the x -polarized THz pump. The induced birefringence $\Delta n = n - n_0 = n_2 I$ is determined from the measurement of the THz induced phase retardation of the probe $\Delta\varphi = \Delta n \omega L/c$ where ω and c are the optical frequency of the probe and the speed of light in vacuum, respectively, I is the FWHM THz intensity (7.2 PW/m^2). L is the interaction length, which has been chosen as Rayleigh length ($L = 410 \mu\text{m}$). For a tightly focused laser pulse, like our THz bullet, the THz intensity drops significantly as we leave the focus, thus making $\Delta\varphi$ localized within the Rayleigh range. As our probe (optical) pulse duration is comparable to the pump (THz) pulse duration, the detected birefringence is a convolution between the THz intensity profile and the optical intensity profile. Figure 1B shows the estimated Δn in comparison with I where Δn is shown to follow the convolution between I and a Gaussian probe pulse intensity profile, confirming the Kerr-like nonlinearity in air. The Kerr-like nonlinearity is instantaneous for all field strengths and no delayed dynamics were observed. The maximum change of refractive index is 1.12×10^{-7} corresponding to a reduction of the phase velocity of the optical pulse by 34 m/s induced by the THz bullet. As the dispersion of our medium is negligible, the group velocity is reduced by the same amount.

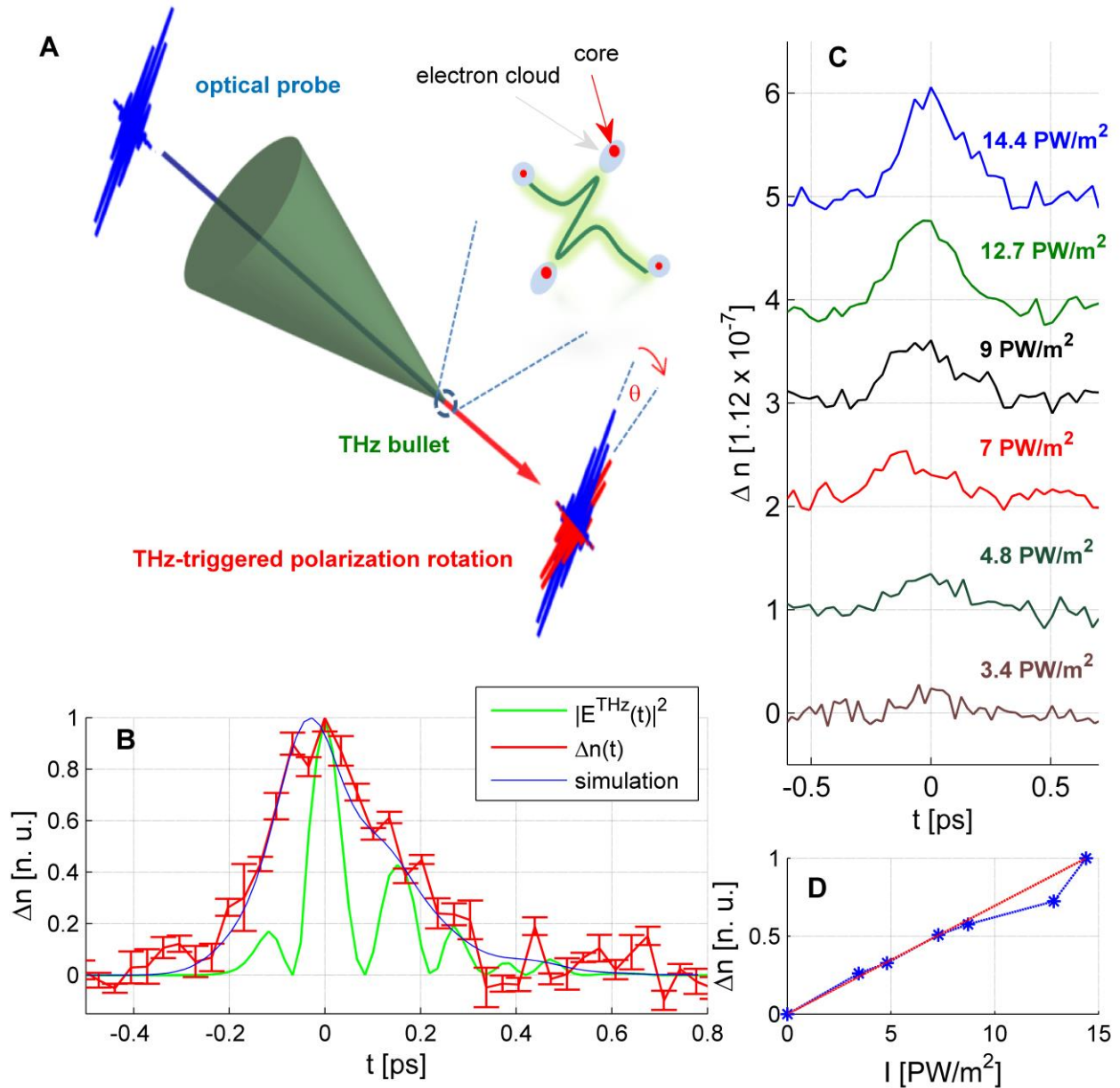


Fig. 1. Terahertz nonlinear manipulation of air. (A) A schematic diagram of the THz-induced nonlinearity. An intense THz bullet nonlinearly deforms (displaces) the electron clouds in the air molecules along its (x -) polarization direction. The near infrared (NIR) probe is initially polarized at 45° from the THz polarization. The probe experiences THz-induced birefringence in air. (b) A comparison between the THz intensity, the measured birefringence $\Delta n = n_x - n_y$ and simulations. The dependence of the measured

birefringence on the triggering THz peak intensity. (D) The birefringence is plotted against the THz peak intensity (blue). A linear fit response (red) is also shown confirming $\Delta n = n_2 I^{\text{THz}}$.

Kerr phase retardation scales linearly with the excitation intensity as shown above. We verified that the excitation levels used here correspond to the linear Kerr regime by measuring the fluence dependence of the induced birefringence. Figure 2C shows the extracted birefringence for various excitation levels down to 25% of the maximum intensity. The time traces show no fluence-dependence change in the temporal response. The maximum birefringence is shown in Fig. 2D against the excitation intensity. Clear linear dependence of the birefringence on the THz peak intensity is observed. This is at the threshold of further applications as the induced change in the refractive index leads to other nonlinear effects such as self-phase modulation, supercontinuum generation, Kerr-induced THz self-focusing and others. At extreme intensities, higher order nonlinear Kerr effects start to play a role, reversing the sign of the refractive index change (3, 16). Such effects manifest themselves in the temporal and spectral responses as well as in violation of the linearity in $\Delta n = n_2 I$, which was not observed here.

We next evaluate the nonlinear coefficient n_2 . In comparison with the optical regime, a single cycle THz pulse carries a very wideband spectrum of several octaves. As the electronic Kerr effect is instantaneous on the THz time scale and the dispersion of our nonlinear medium (dry air) is negligible, the nonlinear response (induced birefringence) should not depend on the excitation frequency. In order to estimate which part of the spectrum is the most effective towards the measured nonlinearity, we employ a set of low pass filters with cut off frequencies (f_{cutoff}) at {18; 6; 3} THz. The peak electric field and intensities from these filters are {3.3; 2.1; 1.1} GV/m and {14.4; 6; 1.5} PW/m², respectively. The THz intensity profiles from these filters are shown in Fig 2A. The original (unfiltered) amplitude spectrum of the exciting pulse is shown in Fig. 2B. Figure 2C shows the measured Δn for different filters, assuming a constant $z_{\text{rayleigh}} = 410 \mu\text{m}$ (assuming a frequency of 2.9 THz, the center of our spectrum extending from 1 to 4.8 THz). In the case

of $f_{\text{cutoff}} = 3$ THz, the field intensity leads to rotation below the sensitivity of our detection (Fig. 1C). Nevertheless, we measured similar birefringence when we used $f_{\text{cutoff}} = 6$ THz and $f_{\text{cutoff}} = 18$ THz. This suggests that the effective spectral content of the applied THz pulse is below 6 THz. The high frequency components are associated with fast temporal oscillations and small spot size in a diffraction limited system (as is the case here (15)). The frequency dependence measurement shows that the effective peak intensity is 6 PW/m^2 contained in < 6 THz (corresponding to an intensity of 3 PW/m^2 at half maximum). The Kerr nonlinear coefficient can thus be deduced as $3.8 \times 10^{-23} \text{ m}^2/\text{W}$ in the Terahertz range. This value compares well with the measurements at the optical frequencies ($2.4 \times 10^{-23} \text{ m}^2/\text{W}$).

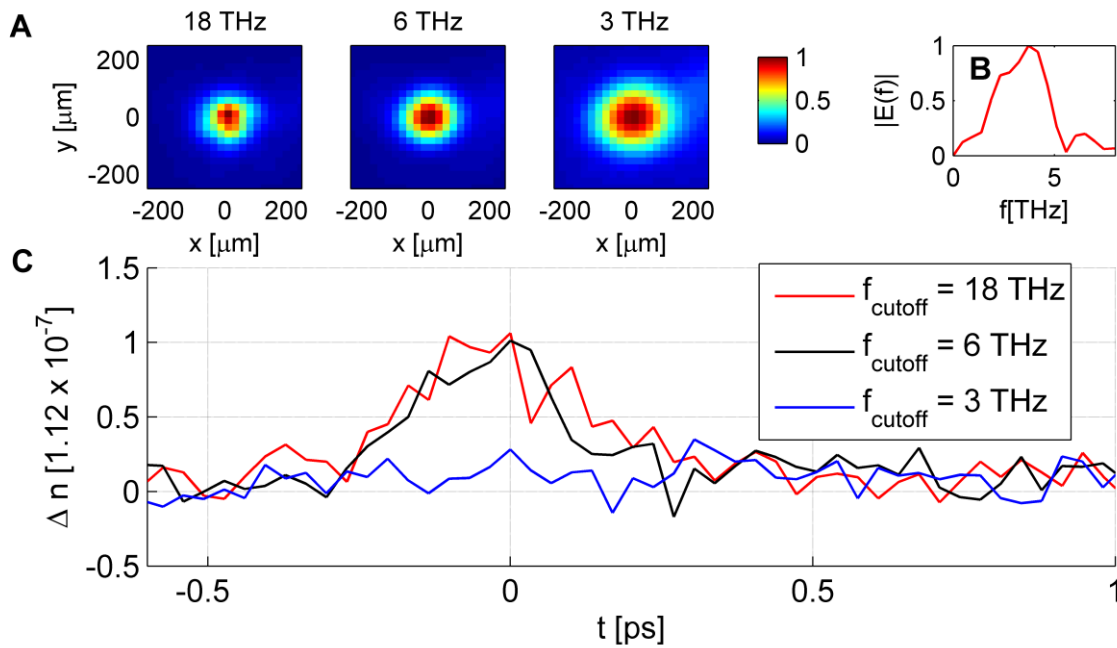


Fig. 2. Spectral dependence of air excitation. (A) the THz spot size at the focus when using low pass filters with cut off frequency of 18 THz, 6 THz, and 3 THz. The corresponding average full width at half maxima are $95 \mu\text{m}$, $117 \mu\text{m}$, and $167 \mu\text{m}$. (B) The amplitude spectra of the exciting THz pulse before filtering. The peak spectral density occurs at 3.9 THz. (C) Frequency-dependent contribution of THz induced birefringence in air. In our experiment, the main contribution for the observed air nonlinearity originates

from carrier frequencies between 3-6 THz where the spectral density of the THz pulse is highest (B).

In conclusion, our results show first low-frequency nonlinear phase phenomena in air, demonstrated using an ultra-intense THz light bullet in a frequency range which was inaccessible for such kind of investigations so far. Quantitatively, the THz-induced nonlinearity is measured to be similar to that at optical frequencies oscillating much faster than the natural time-scale of our THz pulse. Our work opens the door for entirely new THz-induced nonlinear phenomena in air ranging from THz Kerr self-focusing and self-phase modulation to THz solitons and filamentation.

Acknowledgments:

We are grateful to Marta Divall, Alexandre Trisorio, and Andeas Dax for operating the Ti:sapphire laser system. The OPA operation was supported by Carlo Vicario and Marta Divall. The data acquisition software, motors control, and terahertz camera used in this work were previously installed by Carlo Vicario, Clemens Ruchert, Rasmus Ischebeck, Edwin Divall, and Balazs Monoszlai. We acknowledge financial support from the Swiss National Science Foundation (SNSF) (grant no 200021_146769). CPH acknowledges association to NCCR-MUST and support from SNSF (grant no. PP00P2_150732).

1. A. Yariv, *Optical Electronics in Modern Communications* (Oxford University Press, Oxford, 1997).
2. R. W. Boyd, *Nonlinear Optics* (Academic, San Diego, Calif., 1992).
3. V. Lorient, E. Hertz, O. Faucher, B. Lavorel, *Opt. Express* **17**, 13429-13434 (2009).
4. P. L. Kelley, *Phys. Rev. Lett.* **15**, 1005 – 1008 (1965).
5. L. F. Mollenauer, R. H. Stolen, J. P. Gordon, *Phys. Rev. Lett.* **45**, 1095-1098 (1980).
6. M. Mochizuki, N. Nagaosa, *Phys Rev. Lett.* **105**, 147202 (2010).
7. M. Shalaby *et al.*, *Phys. Rev. B* **88**, 140301(R) (2013).

8. T. Qi, Y.-H Shin, K.-L. Yeh, K.A. Nelson, A.M. Rappe, *Phys. Rev. Lett.* **102**, 247603 (2009).
9. L. W. Jie, A. Fallahi, F. X. Kärtner. *Opt. Express* **21**, 9792-9806 (2013).
10. T. I. Oh, Y. J. Yoo, Y. S. You, K. Y. Kim, *Appl. Phys. Lett.* **105**, 041103 (2014).
11. T. Kubacka *et al.*, *Science* **343**, 1333-1336 (2014).
12. H. Y. Hwang *et al.*, *J Mod Optic* (2014). DOI: 10.1080/09500340.2014.918200.
13. C. Vicario *et al.*, *Nat. Photonics* **7**, 720-723 (2013).
14. M. Liu. *et al.*, *Nature* **487**, 345–348 (2012).
15. M. Shalaby and C. P. Hauri. arXiv:1407.1656
16. M. Bache, F. Eilenberger, S. Minardi, *Opt. Letters* **37**, 4612-4614 (2012).